AN ALGORITHM FOR DETECTION OF HIDDEN OBJECTS BY PASSIVE/ACTIVE RADIOMETER

S.I. Ivashov*, A.S. Bugaev, A.S. Turk***, A.V. Zhuravlev***

* Bauman Moscow State Technical University
2-nd Baumanskaya, 5, Moscow, 105005, Russia, sivashov@rslab.ru , +7 (495) 632-22-19
**Moscow Institute of Physics and Technology
**Yıldız Technical University, Istanbul, Turkey

Abstract

Detection of concealed weapons and explosives under people clothing is an actual task nowadays. Different active radar and passive radiometers systems that operate in mm and sub-mm (or THz) bands have been designed for screening passengers in airports. Their effectiveness is rather low at surveying people in outer clothing. The effectiveness could be improved by using dual passive-active radiometer. Such a system consists from the passive radiometer and active noise generator that emits in the same frequency band as the radiometer. The generator is working in stroboscopic mode of operation. This gives an opportunity to record two images (passive and active) simultaneously. An algorithm, that processes both images, has been proposed. It affords to reduce level of false alarms and to raise the contrast of detected objects.

Keywords: radiometer, noise generator, hidden objects.

1 Introduction

The recent advances in both radio frequency and electro-optic components and hardware that could be applied for designing devices operated in millimeter (mm) wave and terahertz band give new opportunities in surveillance of personnel and contraband detection in airports. There is also urgent need to survey people that are going to use ground public transport (metro, buses, trains, and others). This is explained by the fact that the task of air transport defending from terrorists' attacks is mostly resolved. However, ground transport as has been shown by recent events all over the world is the main goal for terrorists. This task is more difficult to solve than in case of air transport because of the need of screening people in outer clothing that is harder to penetrate in microwave band. This is explained by the fact that the attenuation in different types of clothing materials increases with frequency [1].

Numerous research of recent decades have been resulted in designing a few devices of active (radar) [2–4] and passive (radiometer) [5, 6] types. Comparison of these two technologies has been discussed in [7, 8]. In some cases these two technologies are combined to get better results [9, 10].

There is another opportunity to use active/passive radiometer [11, 12]. It consists of passive device (radiometer) and active device (noise generator). The generator emits noise signal in the same frequency band in which radiometer operates. It is worth noting that using of a noise generator has the principal importance because of monochromatic device leads to interference between direct signal to radiometer antenna and reflected one from surveying scene. The experiments with using of monochromatic lighting had demonstrated that the recorded images did not have any likeness to real scene.

2 Theoretical background

Radiometry is in many respects similar to radiolocation. Just as classic radiolocation, radiometry is intended for determination of coordinates of remote objects. The basic distinction between the methods lies in that radar uses its own radiation for illuminating the target. In opposite at detection of objects by the radiometer, the natural radiation of the objects themselves and the sky or artificial generator as the illumination source are used. In this respect radiometry is similar to the passive infrared detectors but uses radio frequencies as the operating range.

It is widely known that the thermal radiation of bodies is super broad band. At temperatures close to 300°K the maximum of the radiation falls on the infrared part of the electromagnetic radiation spectrum. Thanks to this, infrared sensors are widely adopted for the detection of objects under the natural conditions in the night-time. But with the decreasing of ambient temperature the radiation maximum moves to long-wave part of the spectrum. Thus, at temperature of the cosmic microwave background radiation that equals 2,725°K, the radiation maximum is found in the millimeter range (frequency of 160.4 GHz, λ= 1.9 mm) [13].

In quantum mechanics the dependence of the radiation density R_o on its frequency and temperature is given by Planck's law:

$$R_0 = \frac{2\pi f^3 h}{c^2 \cdot \left\{ \exp\left(\frac{hf}{kT} \right) - 1 \right\}} \quad , \qquad (1)$$

where $h = 6.62 \cdot 10^{-34}$ [J·s] is Planck constant,

$c = 3 \cdot 10^8$ [m/s] is the speed of electromagnetic waves in vacuum;

$k = 1.38 \cdot 10^{-23}$ [J·K^{-1}] is the Boltzmann constant;

T [°K] is the absolute temperature of the radiating body;

f [Hz] is frequency;

R_o is the spectral density of radiation equal to power radiated on frequency f in the band of 1.0 Hz by 1.0 sq.m of the radiator.

The frequency f_m on which the spectral density of radiation has the maximum is determined by Wien's displacement law:

$$f_m = 1{,}03 \cdot 10^{11} \cdot T \, . \qquad (2)$$

It follows from Equations (1) and (2) that the spectral density corresponding to $T \approx 300$°K has the maximum in the infrared band, and its value decreases in the range of centimeter and millimeter waves by a factor of several thousands. The attenuation of microwaves in the atmosphere is comparable with that of infrared radiation [14]. Despite the relatively low power of thermal radiation in the microwave range, the sensitivity of up-to-date radiometers is such that the given radiation can be detected at great enough distances [5].

It is worth mentioning that Equation (1) presents the spectral density of radiation R_o for the black-body that is the perfect radiator. For real bodies it will be necessary to make a correction for the emissivity α that is lesser than 1. In the given case

$$R = \alpha \cdot R_o \quad , \qquad (3)$$

where R is the spectral density of radiation of the real body.

It should be also noted that, for the range of Earth's ambient temperatures, the sufficiently complex Planck radiation law (1) could be simplified for computations in the microwave and terahertz bands. Taking into account that for given temperatures and frequencies $hf/kT << 1$, and the exponential member could be expanded into a series, Equation (1) is transformed into the form of

$$R_0 = \frac{2\pi}{\lambda^2} \cdot kT, \qquad (4)$$

where λ is the wavelength of radiation.

Under the real conditions, the radiation flux R_Σ received by the sensor from the examined object will include the component related to the reflection of the outer radiation in addition to its own radiation. At open air, the sky with brightness temperature, that is much lower than the temperature of the ground cover and depends to considerable degree on the state of cloud coverage, can serve as the source of outer radiation [14]. Besides, the illumination can be implemented with the aid of a man-made source. As was mentioned above, a noise signal generator emitting in the operation band of radiometer can be such a source. Given that external sources of illumination are included in to consideration, the spectral density of own and reflected radiation can be presented in the form of

$$R_\Sigma = \frac{2\pi}{\lambda^2} \cdot k \cdot \left(\alpha T + \rho_s T_s + \rho_i T_i \right) , \qquad (5)$$

where ρ_s is object reflectivity of the sky radiation;

T_s is sky brightness (or radiometric) temperature;

ρ_i is object reflectivity of the illumination radiation (noise generator);

T_i is brightness temperature of the illuminating radiation.

Sky brightness temperature especially in cloudless weather at frequency ranges of 40 or 100 GHz is low enough. So, for the outdoor environment the recorded images at these ranges would be influenced by sky brightness temperature. Metal objects are good reflectors. This gives opportunity of metal objects' filtration because of their radiometric temperature is lower in comparison with temperature of the underlying surface. However, in bad weather condition (clouds, rain or fog) the sky temperature at 250 GHz is significantly higher due to increased atmospheric absorption. In worst case of high humidity, the sky illumination can be removed from consideration entirely [5].

A diagram of receiving of the radiometric signals of various origins that radiated and reflected by the object is presented in Fig. 1. This figure also demonstrates the principal arrangement of the devices on a land carrier that includes radiometer and noise illumination generator. The main lobe of the generator's antenna pattern has to be wider than that of the radiometer antenna. The noise generator and the radiometer are uniaxially anchored on the scanning device to ensure the survey of a terrain sector in front of movement of the land carrier along an azimuth. A line-by-line scanning is provided thanks to movement of the carrier. Such a selection of the parameters and positioning of the devices assures the condition of uniform illumination by the noise generator of a section of the ground surface observed by the radiometer antenna.

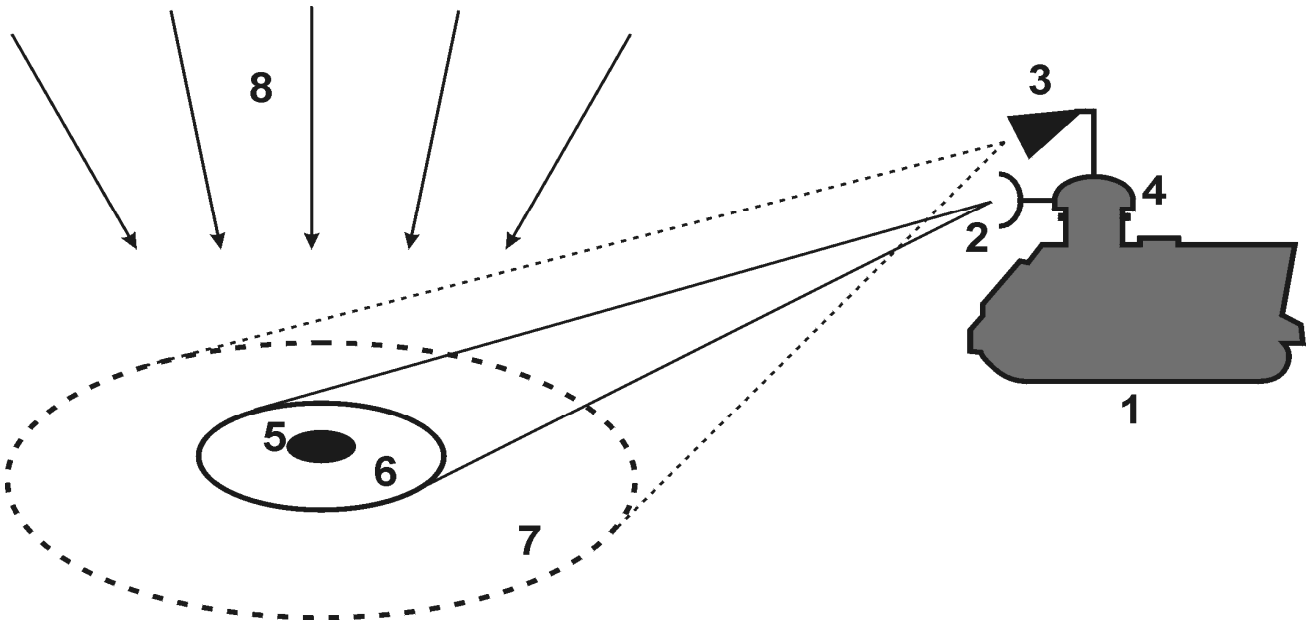

Figure 1. Principal arrangement of passive/active radiometer

1 — equipment carrier;
2 — radiometer antenna;
3 — antenna of noise generator (illuminator);
4 — scanning device;
5 — object on ground surface;
6 — observing sector of main lobe of radiometer antenna on ground surface;
7 — sector of ground surface radiated by antenna of noise generator;
8 — sky radiation.

In the general case the reflectivity of sky radiation ρ_s and illumination radiation ρ_i differs from each other. This is related to the form of the reflecting body. Since the sky radiation is scattered and illuminates an object from the upper hemisphere more or less uniformly, the radiation reflected by the object will be omnidirectional. The illumination radiation is directed away from the noise generator, and the object of the flat form may reflect it away from the receiving radiometer antenna. In this case ρ_i would be equal to zero.

3 Experimental installation

An experimental radiometric complex of the 8-mm wave range was developed to check the possibility of detection of metal objects on the underlying surface. General view of the passive/active radiometer is shown in Fig. 2. As objects for detection, TM-62M land antitank mines with metal casing were selected.

The selection of the wave range was related to the fact that high contrast of anti-tank mines installed on the ground surface can be provided in this range with an acceptable aperture of a radiometer antenna. The employment of a passive-active mm wave radiometer was proposed to improve the detection parameters. The complex included an 8-mm wave range radiometer, a noise generator of the same range and a TV camera. All these devices were coaxially secured at a mechanical appliance, which provides for scanning in two planes: according to the elevation angle and to the azimuth.

By doing so, the possibility of survey in a terrain sector from a fixed carrier was ensured. The main lobe of the radiometer antenna was 1.0 deg and of the noise generator antenna — about 10.0 deg. The relative positions of the generator and radiometer antennas were selected in such a way that the minimum level of the direct signal from the noise generator to the radiometer antenna was achieved. The TV camera allowed an operator to compare images obtained in the microwave and visual ranges.

Figure 2. General view of experimental installation

As was previously noted the usage of the noise generator with the spectrum filling the entire operation band of the

radiometer in the capacity of a terrain illumination source is a must. Otherwise the image recorded by radiometer is random in character and cannot be identified with the observed objects if a monochromatic generator is used. This is because of coherent summation of the signals reflected from the observation object and the direct transmission of the signal from the noise generator to the radiometer's receiving antenna. The result of this summation depends on phase of reflected signal that is unpredictable in his nature.

The operation of the equipment provides for simultaneous generation of two images: one in the passive mode when the noise generator was switched off and the other one in the active mode when the illuminator was switched on.

The picture of a proving ground is seen in Fig. 3. Nine metallic anti-tank mines of TM-62M type were laid in three staggered rows on the ground surface in the foreground. The distances from the nearest and most distant mines to the radiometric complex were 10.0 and 22.0 m, respectively. The mines in the right row were installed on supports and inclined towards the radiometric installation to enhance contrast.

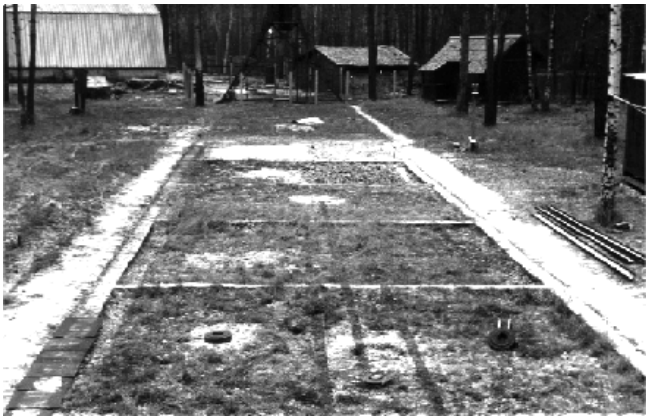

Figure 3. General view of the ground test-bed with mines

The row of metallic plates can be seen in the left bottom corner of the picture. At the background of the picture a metal tower (in the center) and a corrugated metal roof (in the left corner) are visible.

4 Experimental results

The results of survey of the terrain in the passive mode and in the mode with illumination are illustrated in Figs. 4 and 5, respectively. Gradations of brightness in these figures are chosen so that darker sections of image correspond to objects with lower radiometric temperature. Since metal objects have reflectivity about 1 in the microwave range, they look darker on the radiometric image. This is because metal surface reflects the sky radiation which brightness temperature is lower than the temperature of the ground cover.

Fig. 4 clearly demonstrates the left mine nearest to the radiometer and the mines of the right row the contrast of which is higher. The row of metallic plates is seen to the left of the minefield, and the metal roof of a building and the outline of a tower are clearly visible in the background. The produced image shows that the contrast of mines laid in parallel to the ground surface is sufficient for their detection at a distance up to 15.0 m only for the specified parameters of the radiometric sensor in the passive mode. At greater distances their contrast lies at the level of the natural variations of brightness temperature of the underlying surface.

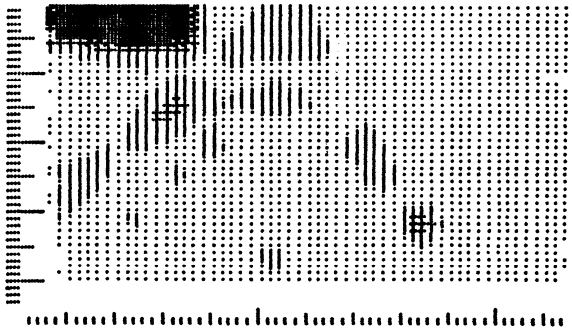

Figure 4. Passive radiometric image of the ground test-bed

When the noise generator is switched on, the image changes qualitatively. The contrast of metal objects with respect to the background depends not only on the type of the surface but also on the shape of objects observed. Thus, flat objects, which reflect the radiation of the noise generator with a high brightness temperature like a mirror, can be viewed in the image as objects having low brightness temperature. It can be explained by the fact that the sky radiation alone is reflected in the direction of the radiometer antenna. The metal roof of the building and the metal plates used as a reference mark are such objects in the image.

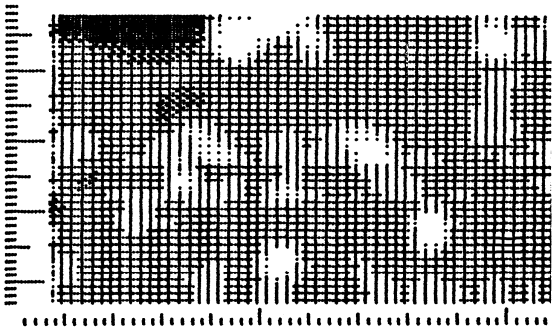

Figure 5. Active radiometric image of the ground test-bed with noise generator being switched on

The metal objects of complex shapes, being sets of bright points, reflect the illuminator radiation in the direction of the radiometer antenna as well. Such objects change the contrast relative to the background when the noise generator is switched on. The active radiometric image of the same scene is presented in Fig. 5. The mines and tower change their contrast but the row of plates and the corrugated roof keep contrast in this picture. Various reflections from local objects on the ground can also be seen.

Analysis of the passive and active radiometric images gives possibility to make some conclusions. Contrast of metal objects on passive radiometric image is not enough for their reliable detection at long distance. Oppositely, on active image the mine contrast is high enough but level of false alarms is high also.

For the selection of complex-shaped objects like mines an algorithm was proposed which operates in accordance with a scheme of coincidences and separates only those objects in the images that change their contrast relative to the background when the illuminator is switched on. Fig. 6 demonstrates effectiveness of the proposed algorithm.

Figure 6. Results of co-processing images in Figs. 4 and 5

In this picture, only six mines and the tower are visible. All the other objects have disappeared from the image. This algorithm is more effective for metal object detection and differs from one proposed in [11] where had been proposed to subtract the passive and active images to enhance contrast.

Conclusion

It is necessary to note that the proposed method of detection of objects that have complex form can also be used for other tasks, for example it could be used to detect weapons and explosives under people clothing. For this purpose the noise generator should operate as a stroboscope. Thus, when the noise generator is switched off and the radiometer antennas are in fixed positions, an element of the passive radiometric image will be registered, but when the mentioned generator is switched on, an element of the active radiometric image will be recorded. With proper selection of the switching frequency of the noise generator, a complete matching of both images can be obtained in the course of their subsequent processing.

Acknowledgements

This work was supported by the Russian Foundation for Basic Research, and the Scientific and Technological Research Council of Turkey.

References

[1] R. Appleby, H.B. Wallace. “Standoff Detection of Weapons and Contraband in the 100 GHz to 1 THz Region”, *IEEE Transactions on Antennas and Propagation*, Vol. 55, No. 11, pp. 2944–2956, November 2007.

[2] D.M. Sheen, D.L. McMakin, W.M. Lechelt, J.W. Griffin. “Circularly polarized millimeter-wave imaging for personnel screening”, *Passive Millimeter-Wave Imaging Technology VIII, Proceedings of SPIE*, Vol. 5789, pp. 117–126, 2005.

[3] D.L. McMakin, P.E. Keller, D.M. Sheen, T.E. Hall. “Dual surface dielectric depth detector for holographic millimeter-wave security scanners”, *Passive Millimeter-Wave Imaging Technology XII, Proceedings of SPIE*, Vol. 7309, pp. 73090G 1–10, 2009.

[4] K.B. Cooper, R.J. Dengler, N. Llombart, T.Bryllert, G. Chattopadhyay, E.Schlecht, J. Gill, C. Lee, A. Skalare, I. Mehdi, P.H. Siegel. “Penetrating 3-D Imaging at 4- and 25-m Range Using a Submillimeter-Wave Radar”, *IEEE Transactions on Microwave Theory and Techniques*, Vol. 56, No. 12, pp. 2771–2778, December 2008.

[5] C. Mann, “Real time passive imaging at 250GHz for security: Technology and phenomenology”, *International Conference on Electromagnetics in Advanced Applications, ICEAA '09*, pp. 1013–1015, 2009.

[6] R. Doyle, B. Lyons, J. Walshe, P. Curtin, A.H. Lettington, T. McEnroe, J. McNaboe. “Low Cost Millimetre Wave Camera Imaging up to 140GHz”, *34th European Microwave Conference*, Amsterdam, pp. 1285–1288, 2004.

[7] H.B. Wallace. “Analysis of RF imaging applications at frequencies over 100 GHz”, *Applied Optics*, Vol. 49, Issue 19, pp. E38–E47, 2010.

[8] H.B. Wallace, M.J. Rosker, “Analytical performance comparison of active and passive SMMW imaging for contraband detection”, *Proceedings of SPIE*, Vol. 7485, 74850E, pp. E1–E13, 2009.

[9] Bolten, J.D.; Lakshmi, V.; Njoku, E.G. Soil moisture retrieval using the passive/active L- and S-band radar/radiometer, IEEE Transactions on Geoscience and Remote Sensing Vol. 41, Issue 12, pp. 2792–2801, 2003.

[10] Yan Jin-Hai; Li Xing-Guo; Wang Ming, “MMW collocated detectors by fusing active and passitive detection”, *Proceedings of the Fifth International Conference on Information Fusion*, Vol. 2, pp. 1416–1421, 2002.

[11] F.J. Poradish, “Ka-Band Passive/Active Airborne Radar”, *Proc. of the IEEE Nat. Aerospace and Electron. Conf.*, NAECON’82, pp. 1262–1269, 1982.

[12] A.A. Dmitrienkov, S.I. Ivashov, V.N. Sablin, B.A. Ufraykov . “Passive-Active MM Wave Radiometer for Detection of Mines installed on the Ground Surface”, *Proc. of the 5th International Conference on Radar Systems.* Oral Session 1.7, May 17–21, Brest, France, 1999.

[13] D.J. Fixsen. “The Temperature of the Cosmic Microwave Background”, *The Astrophysical Journal*, Vol. 707, No. 2, pp. 916–920, 2009.

[14] Preissner J., “The influence of the atmosphere on passive radiometric measurements,” *Symp. Millimeter and Submillimeter Wave Propagation and Circuits, AGARD Conf. Proc.*, no. 245, pp. 48/1–48/13, 1972.